Applied Catalysis B: Environmental 221 (2018) 1–8

Contents lists available at ScienceDirect

Applied Catalysis B: Environmental

journal homepage: www.elsevier.com/locate/apcatb

Analysis of photoefficiency in TiO_2 aqueous suspensions: Effect of titania hydrodynamic particle size and catalyst loading on their optical properties

J. Carbajo[a], A. Tolosana-Moranchel[b], J.A. Casas[b], M. Faraldos[a], A. Bahamonde[a,*]

[a] Instituto de Catálisis y Petroleoquímica, ICP-CSIC, Marie Curie 2, 28049 Madrid, Spain
[b] Sección de Ingeniería Química, Facultad de Ciencias, Universidad Autónoma de Madrid, C/Francisco Tomás y Valiente 7, 28049 Madrid, Spain

ARTICLE INFO

Keywords:
Photocatalysis
TiO_2
Hydrodynamic particle size
Optical properties
$HO^{\bullet}$ generation

ABSTRACT

Effect of TiO_2 hydrodynamic particle sizes and catalyst loading on the optical properties of three commercial photocatalysts has been analyzed (P25 Aeroxide®, P25/20 VP Aeroperl® and P90 Aeroxide®). These catalysts, characterized by similar structural and electronic properties, but with singular differences in morphology and aggregation particle sizes, have been studied to understand the corresponding crossed effects on their final photo-efficiencies throughout organic matter removal in aqueous suspensions, with a pollutant such as phenol, where photo-oxidation is regularly described as mediated by an indirect photo-mechanism via $HO^{\bullet}$ radicals. Reflectance measurements in the range of visible wavelength, close to TiO_2 absorption edge, could be comparable to extinction coefficient in the UV-A range and may well be suitable to optimize catalyst loadings. Phenol photocatalytic efficiency followed P25 > P90 > P25/20 order, emphasizing that increases in TiO_2 hydrodynamic particle sizes are detrimental to phenol photo-efficiency, and highlighting that radiation–photocatalyst interactions are essential but not enough to guarantee an improved photodegradation rate. Finally, the higher values of $HO^{\bullet}$ found in sonicated P25/20 catalyst could corroborates its better performance in phenol photodegradation, as a consequence of lowest hydrodynamic particle sizes in reaction media, which take advantage of light as a result of a significant increase in exposed surface area.

1. Introduction

Semiconductor nanomaterials constitute a very attractive and rising technology for treatment of wastewater with moderate content of organic pollutants, and compose a highly sustainable alternative when solar light is used as the primary source of energy [1–3]. Particularly, TiO_2 photocatalysts are widely used in solar assisted photocatalytic processes to achieve environmental remediation and water splitting as a consequence of their low cost, low toxicity, and good stability and performance [4].

Nevertheless, it is well known that rate and efficiency of heterogeneous photocatalytic reactions is highly dependent on different parameters, such as initial concentration of pollutants, mass of catalyst, pH, temperature, radiant flux or oxidant concentration, which govern the kinetic of the process [3,5]. However, unlike conventional heterogeneous catalytic processes, it must be also taken into account that photocatalytic treatments are mediated by photonic activation [5]. Moreover, final photoefficiency of every single photocatalyst in aqueous suspensions also depends on their physico-chemical properties (e.g. exposed surface area, particle aggregation, crystal phase and size, amount of structural defects, etc.), which in turn can also be affected by chemical nature of pollutants and aqueous environments [6,7].

Many works have frequently tried to analyze the complex effect of the most relevant catalyst properties and reaction parameters on final photo-efficiency. Among those, it can be emphasized the influenced by the surrounding operational conditions [6,8,9] and mostly the related to TiO_2 physico-chemical properties [6,10,11]. Surely, titania encounters some environmental factors in practical applications (ionic species, natural organic matter, sunlight, etc.), where inevitably undergo physical and chemical transformations, due to its high surface reactivity and exposed surface area [12]. These noted titania behaviors have been usually related in the literature to aggregation process [13–15], where e.g. hydroxyl groups of titania surfaces could interact with different components in aqueous solutions causing particle aggregation; or even changes in pH values along photocatalytic process could generate some particle aggregation. So, these TiO_2 interactions in aqueous suspensions undoubtedly led to different photo-reactivity performances, with particular dependence on titania aggregate sizes and morphological structure in aqueous solutions [12]. For that, an in-depth understanding of the effect of nano-TiO_2 transformations in

* Corresponding author. Tel.: +34 915855475; fax: +34 915854760.
E-mail address: abahamonde@icp.csic.es (A. Bahamonde).

http://dx.doi.org/10.1016/j.apcatb.2017.08.032
Received 13 June 2017; Received in revised form 4 August 2017; Accepted 10 August 2017
Available online 26 August 2017

aqueous irradiated suspensions is essential in assessing their photo-reactivity and environmental behavior.

In this context, this work aims to explore the significant role that might be playing some of the different TiO_2 catalyst properties throughout organic matter removal in aqueous suspensions. Specifically, the analysis of potential relationship between TiO_2 optical properties and hydrodynamic particle size in aqueous environment on final photocatalytic-efficiency has been carried out for three commercial nanostructured TiO_2 catalysts: P25 Aeroxide®, P25/20 VP Aeroperl® and P90 Aeroxide®, with the similar structural and electronic properties but with singular differences in morphology and aggregation particle size. For this purpose, the optical properties of TiO_2 aqueous suspensions, following different experimental methodologies, proposed by previous authors [16,17], and its relationship with the optimal catalyst loading and titania hydrodynamic particle size have been established. Finally, to try to understand the significant effect of TiO_2 particle sizes and their aggregation phenomena on photocatalytic efficiency in aqueous environment, a study of sonication pre-treatment, before phenol photodegradation, joined to an analysis of hydroxyl radical production has been also carried out.

2. Experimental

2.1. Photocatalysts and chemicals

Photocatalytic runs were performed using three different commercial TiO_2 catalysts: the well-known P25 Aeroxide® titanium dioxide, extensively used as standard titania in heterogeneous photocatalysis [18], a granulated version of this P25 catalyst, denoted as P25/20 VP Aeroperl®, and P90 Aeroxide®, with higher surface area, all of them provided by Evonik company.

Analytical grade phenol was purchased from Panreac. All reagents used for chromatographic analyses, Milli-*Q* water, *ortho*-phosphoric acid, methanol, sulphuric acid and sodium carbonate, were HPLC grade from Scharlab.

2.2. Photocatalysts characterization

Structural characterization of these catalysts were performed with an X-ray poly-crystal diffractometer PANalytical X'Pert PRO using nickel-filtered Cu*K*α (1.541874 Å) radiation, operating at 40 kV and 40 mA, 0.02° step size and 50 s per point of accumulating time; crystal size was estimated by employing the Scherrer equation [19]. Nitrogen adsorption–desorption isotherms measurements were obtained at 77 K in a Micromeritics Tristar; samples were previously outgassed overnight at 413 K and vacuum of $< 10^{-4}$ Pa to ensure a dry and clean surface free from any loosely adsorbed species and, specific surface areas were determined by the BET method [20].

Scanning electron microscopy (SEM) analyses were performed to determine morphology of the studied TiO_2 powders (S-3000N, Hitachi).

Laser diffraction (LD) measurements were carried out in a Mastersizer S, Malvern Instruments, to characterize the hydrodynamic particle size distributions in aqueous suspensions. Diameters or volumes of TiO_2 aggregates in water suspensions were provided by measuring the intensity of a scattered He–Ne laser (λ = 632.8 nm) beam passing through dispersed and stirred TiO_2 aqueous suspensions. These measurements were acquired by systematically adding to the suspension the amount of catalyst to obtain obscurance values around 20% for a comparison study among all studied catalysts. This technique also provided values for available catalyst surface area, which were calculated taking into account TiO_2 particle size distribution, and assuming spherical shape of the aggregates.

UV–vis diffuse reflectance spectra of the photocatalysts powders were registered in a Cary 5000 Agilent spectrometer equipped with integrating sphere (Spectralon® PTFE was used as reference). Band-gap was determined by Tauc plot using the equation $\alpha h\nu = A(h\nu - Eg)^{n}$ [16], where $h\nu$ means energy, α is the absorption coefficient, A is a constant called the band tailing parameter, Eg is the energy of the optical band gap and n is the power factor of the transition mode and depends on type of band-to-band transition, which can take on values of 3, 2, 3/2, or 1/2, corresponding to indirect (forbidden), indirect (allowed), direct (forbidden), and direct (allowed) transitions, respectively. Finally, optical properties of catalysts suspensions were studied following the methodology proposed by Cassano et al. [17,21,22] and adapted by Plantard et al. [23]. Optical properties (extinction, absorbance and spectral diffuse reflectance) measurements were performed at the experimental setup described in Supporting information Fig. 1. In the case of absorbance and reflectance measurements the sample cell (optical length, 2 mm and 1 cm, respectively) was placed on a magnetic stirrer and lined up entrance and output of integrating sphere, respectively (Milli-*Q* water and PTFE was used as reference). Extinction measurements were completed using a 2 mm optical length sample cell, placed far from detector position, without integrating sphere, introducing a narrow slit detector to minimize collected out-scattered radiation. All measurements were performed on freshly prepared and non-sonicated suspensions at different catalyst loadings. Under these studied conditions, suspensions were rather stable and fairly reproducible. In all cases suspensions were stirred during every measurement.

2.3. Photocatalytic activity

Photodegradation runs were carried out in a stirred 1 L Pyrex semi-continuous slurry photoreactor set in a Multirays apparatus (Helios Italquartz), described in deep detail in [24], at atmospheric pressure and room temperature, employing oxygen as oxidant agent. This Multirays apparatus is constituted by a camera whose internal surface is covered by a highly reflectant metal sheet to guarantee a better use of the light, where 10 fluorescent lamps of 15 W each are distributed. Two types of fluorescent lamps were employed: Black Light Blue lamps (Narva LT 15W/073 Black Light Blue, BLB) that present a band emission at UV-A region, centered at 360 nm, and daylight fluorescent lamps (Narva LT 15W/865 Cool Daylight, DL) which emit on visible range with a spectrum distribution closed to solar. The total irradiance was measured by a Kipp & Zonen, model CUV-4, broadband UV radiometer in UV-A range (306–383 nm).

Different operational conditions were employed to analyze the photocatalytic activity of phenol. The influence of catalyst loading (25–1500 mg L^{-1}) was carried out with all the studied TiO_2 catalysts at an initial phenol concentration of 50 mg L^{-1} and 38.4 W m^{-2} of irradiance.

Phenol and aromatic intermediates were identified and quantified by high performance liquid chromatography, HPLC (Varian 920 LC) with photo-diode array detector, using Nucleosil C18 column (150 × 4.6 mm, 5 μm) as stationary phase at 40 °C. Mobile phase flow was 0.8 mL min^{-1} of 20/80% v/v methanol/acidic water (0.1% phosphoric acid) mixture. Total organic carbon (TOC) content of aqueous samples was also determined throughout all the experiments with a TOC-$V_{CSH/CSN}$ Shimadzu analyzer. All the samples were filtered with a 45 μm PTFE membrane previously to the analyses.

Inlet radiation flux was calculated through ferrioxalate actinometry runs by applying the reactor mass balance [25–28].

Sonication pre-treatment was performed using 0.250 g L^{-1} of titanium dioxide suspensions and dispersed during 1 h in a soundproof cabin using a 100 MHz tip (Misonix Microson 2000XL).

2.4. Hydroxyl radical production

Hydroxyl radical generation ($HO^{\bullet}$) was measured using terephthalic acid (TA) in alkaline solutions [18,19], which has been found to be a selective free hydroxyl radical probe, producing 2-hydroxy terephthalic acid (TAOH); this procedure has been extensively used to evaluate the ability of TiO_2 to generate hydroxyl radicals [29]. 0.25 g L^{-1} of TiO_2

and 0.5 mM of TA were mixed in a suspension where NaOH 2 mM was previously dissolved. After that, the mixture was stirred and irradiated in 1 L photo-reactor used in this work. Fluorescence emission of 2-hydroxyterephthalic acid (TAOH) was measured at wavelength of 425 nm and an excitation wavelength of 315 nm using a Perkin Elmer Luminescence spectrometer LS 50B, allowing measurements of free hydroxyl radicals in solution.

3. Results and discussion

3.1. Characterization studies

The X-ray diffraction (XRD) patterns (not shown here) revealed that all these TiO_2 photocatalysts (P25, P25/20 and P90) nearly presented same anatase/rutile crystal structure [28]. Calculated anatase/rutile ratios, around 86/14 with identical crystallite sizes of anatase and rutile for P25 and the P25/20, 21 and 33 nm, respectively, were assessed; whereas in the case of P90 slightly lower crystallite sizes of anatase and rutile were estimated (17 and 29 nm, respectively).

Scanning electron microscopy (SEM) and N_2 adsorption–desorption isotherms were performed in order to characterize morphological and textural properties of these studied TiO_2.

The corresponding adsorption–desorption isotherms of these Evonik powder nanoparticles showed that all these photocatalysts are non-mesoporous materials and present type II isotherms (see Supporting information Fig. 2), according to *t*-plot, no micropores were either detected. Consequently, porosity of these TiO_2 photocatalysts becomes generated by inter-particle spaces causing macroporosity [30]. Whereas identical values of surface area (S_{BET}) were obtained for both P25 and P25/20 catalysts (55 $m^2\,g^{-1}$), P90 TiO_2 exhibited significantly higher specific surface area (81 $m^2\,g^{-1}$).

Fig. 1 summarize SEM micrographs, where P25 and P90 images reveal the presence of non-compacted and irregular aggregates in the range of 1–2 μm (Fig. 1A and B), whereas higher magnifications (Fig. 1D and E) show heterogeneous aggregates of TiO_2 nanocrystals of several nm in size, where slightly lower crystal sizes seem to characterize P90 catalyst (Fig. 1E), in agreement with the reported XRD results [26]. On the contrary, the granulated Aeroperl® P25/20 TiO_2 (Fig. 1C and F) presents indeed, a much more compacted spherical and bigger homogeneous aggregates, where a clearly bimodal distribution apparently define the exposed aggregation state, constituted by smaller spherical particles in the ~1–4 μm range and a more significant size contribution estimated around ~20–30 μm.

These above characterization results are also pointing out that the secondary particles sizes found in P25/20 catalyst do not affect S_{BET} (54–55 $m^2\,g^{-1}$ as P25 as P25/20) and, as it was previously reported for P25 TiO_2 [31], BET surface area should respond more directly to the primary particle size (crystal sizes) rather than secondary particle sizes (aggregates). So, the higher surface area found in P90 TiO_2 (81 $m^2\,g^{-1}$) seems to be more related to its slightly smaller anatase and rutile crystal sizes (17 and 29 nm, respectively).

Even if the aggregation state could be evaluated by SEM studies, particle size in aqueous suspensions may differ from the determination in dry conditions. Laser diffraction (LD) analyses were carried out in order to obtain the hydrodynamic particle size for P25, P90 and P25/20 catalysts in aqueous suspension, which could be defined as the "mean particle size" in aqueous media, where some particle aggregation must be expected [32]. These measurements make possible to determine the real titanium dioxide size in the aqueous reaction media. Representative distribution curves of TiO_2 particle sizes in deionized water suspension at pH 5.8–6.0 (corresponding to natural pH of phenol photodegradation runs) are showed in Fig. 2. These data suggest that both, P25 and P90 powders are constituted by a mono-modal distribution where the maximum contribution is observed at ~3.5 μm for P25, while slightly smaller aggregates are found for P90 TiO_2 (~2.8 μm). By contrast, concerning the aggregated material, P25/20 TiO_2 shows a much larger hydrodynamic particle size distribution, characterized by one smaller shoulder around 3 μm (such as P25) and an important relevant contribution centered in ~37 μm. As it may be noted from these analyses, LD results are fairly consistent with SEM images (see Fig. 1).

3.2. Influence of optical properties, hydrodynamic particle size and catalyst loading on photo-oxidation rate

In previous studies [33], two conventional operational parameters such as pollutant concentration and radiant flux were analyzed with the well-known P25 TiO_2 Aeroxide®, used as standard titania in many heterogeneous photocatalysis studies [20]. A radiant flux of 38.4 W m^{-2} in UV-A range was chosen as the most appropriate setup to

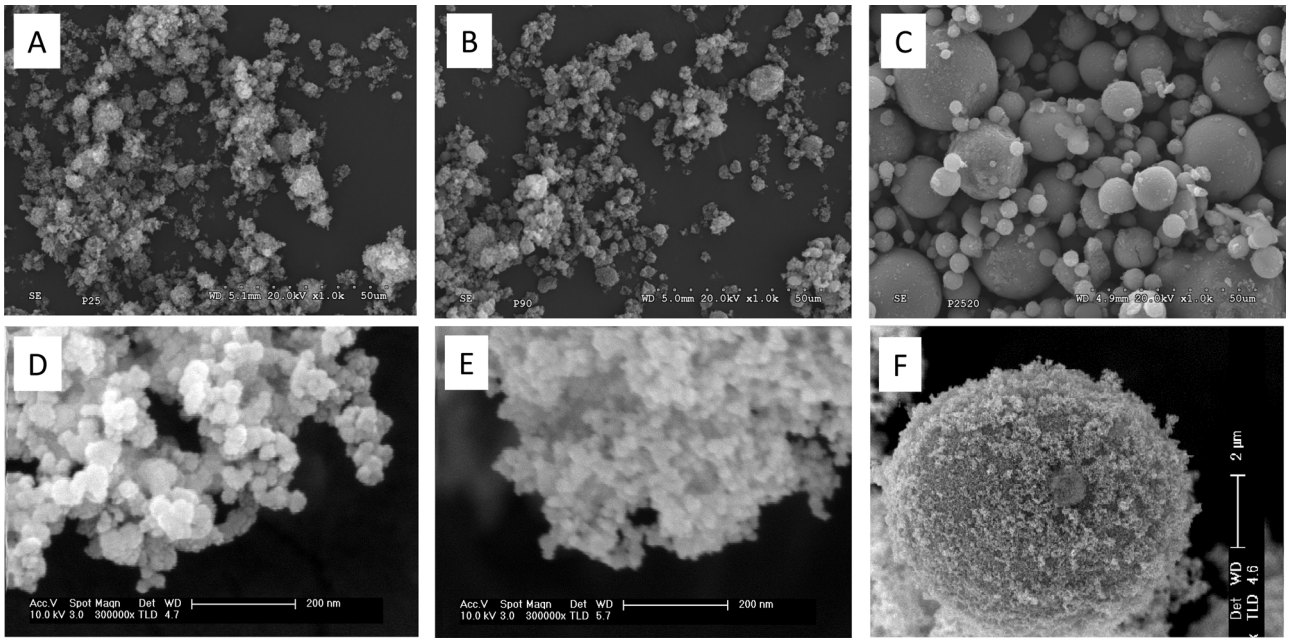

Fig. 1. SEM micrographs: (A and D) P25, (B and E) P90 and (C and F) P25/20.

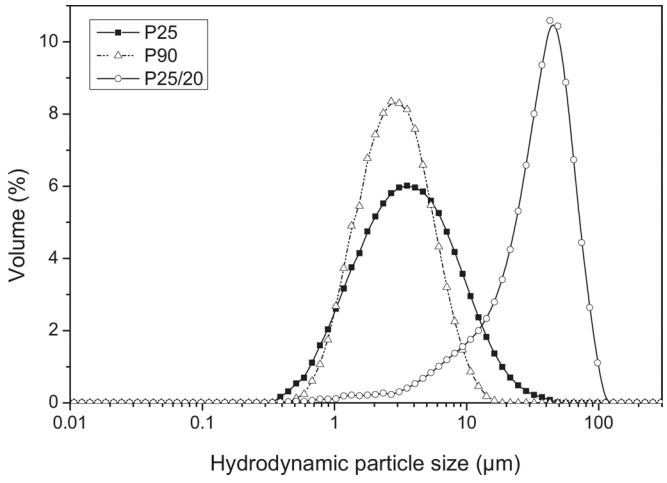

Fig. 2. Hydrodynamic particle size distributions of original TiO_2 photocatalysts in aqueous suspensions.

(i) obtain a good balance between number of photons reaching TiO_2 photocatalyst surface and photodegradation reaction rate, where initial phenol rates were close to the range of proportionality to $E_{UV\text{-}A}$ and (ii) work at a total radiant flux in the UV-A range close to the typical average solar UV flux values, was found to be 30 $W_{UVA}\,m^{-2}$ [34]. Second, all studied initial phenol concentrations (50 mg L^{-1}) demonstrated to be in the optimum range for the photocatalytic performance in this photoreactor.

Taking into account most authors agree that the rate of photo-mineralization of organic pollutants with irradiated TiO_2 follows more or less the L–H law, where rate constants and orders are only "apparent" [3,24]; TOC reaction rate becomes constant and independent of initial phenol concentration, being able to be simplified to a pseudo-zero-order kinetic equation [3,24], at the same time, a pseudo-first-order kinetic model could be considered to describe phenol photo-oxidation rate.

In this context, influence of catalyst loading on initial TOC photodegradation rate for P25, P25/20 and P90 catalysts is given in Fig. 3. Although some different behaviors can be seen for each single catalyst, initial TOC photodegradation rates always increase with catalyst loading until a certain value, from which it remains almost invariable. While P25 and P90 catalysts have arisen maximum values at low catalyst loadings (~0.20–0.50 g L^{-1}), nearly two times higher catalyst loading (~0.7–1.0 g L^{-1}) was necessary in the case of P25/20 to get

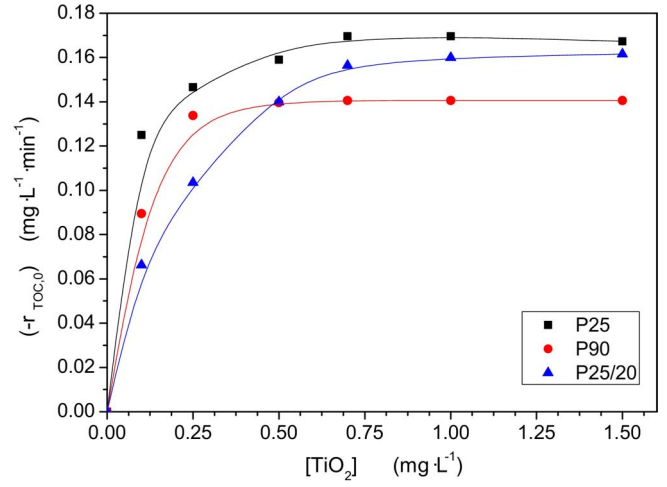

Fig. 3. Influence of TiO_2 catalyst concentration on initial TOC photodegradation rate. Operating conditions: $[phenol]_0$ = 50 mg L^{-1}, pH_0 = 6.0, irradiance = 38.4 W m^{-2}, Q_{aire} = 75 mL N min^{-1}.

maximum initial photodegradation rates.

As it is well known, the optimum catalyst loading mainly depends on their optical properties, where the sizes of illuminated TiO_2 particles play a key role on the photocatalytic activity [35]. At low catalyst loadings [$(TiO_2) < 0.5$ g L^{-1}], phenol photodegradation rates are considerably higher for P25 and P90 catalysts than for P25/20, meaning that TiO_2 catalysts characterized by lower homogeneous particle size in water suspension, P25 and P90, are reaching maximum efficiency at low catalyst loadings. So, according to Fernández-Ibáñez et al. [32] the above obtained results could be explained by: (i) the lower mean hydrodynamic particle sizes of P25 and P90 catalysts allow a better exposition of aqueous suspended particles surface facilitating pollutant access to the photo-generated species (ii) at the same catalyst loading, TiO_2 P25/20 presents a lower number of aggregates in water suspension (higher hydrodynamic particle size), reducing the exposed surface, the radiation absorption capacity and, limiting the access of pollutant reactants and light to the internal catalyst particles.

The determination of radiation profiles inside the used photoreactor was previously estimated and reported [36], where the different catalyst loadings needed to reach the maximum initial TOC photodegradation rates depends on the TiO_2 optical properties. The studied photocatalytic systems exhibit high scattering/extinction ratio (albedo coefficient, ω) even when absorption takes place. That is why a good solution, instead of using the extinction coefficient, is to measure the scattered radiation at higher wavelengths, where absorption does not occur and extinction and scattering are the same. In Fig. 4, albedo coefficient, which indicates the ratio of radiation scattered to radiation extinguished by the catalyst, as a function of mean diameter of hydrodynamic particle size is given for these three TiO_2 photocatalysts between 345 and 390 nm.

Following, the percentage of reflected radiation is shown as a function of the catalyst concentration in Fig. 5, where radiation at 420 nm scattered can be assimilated as the radiation attenuation provoked by TiO_2 particles. It can be noticed that all these data describes a similar trend to those depicted in Fig. 3, in which the initial photodegradation rate and the reflected radiation increase until they reach a plateau at a given catalyst concentration, due to the fact that above that concentration the maximum amount of radiation is extinguished. Even though optimum catalyst loading in these two figures don't match because of a different path length between photo-reactor and the measurement cell, scattering measurements at above absorption can well predict the optimal catalyst loading of different aggregation systems.

To point out this fact, profiles of incident radiation available (G) along the reactor diameter were plotted in Supporting information Fig. 3. The incident radiation was calculated solving the radiative transfer equation (RTE) by using the discrete ordinates method (DOM) [21,22] from the scattering and absorption coefficients reported

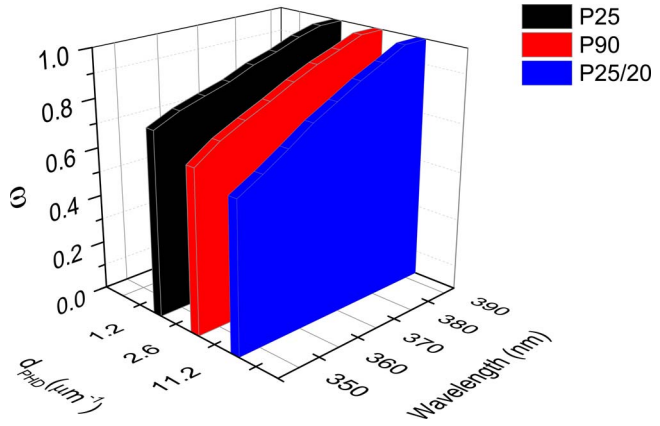

Fig. 4. Albedo coefficient at λ = (345–390) nm, with mean diameter of hydrodynamic particle in aqueous suspensions (d_{PHD}).

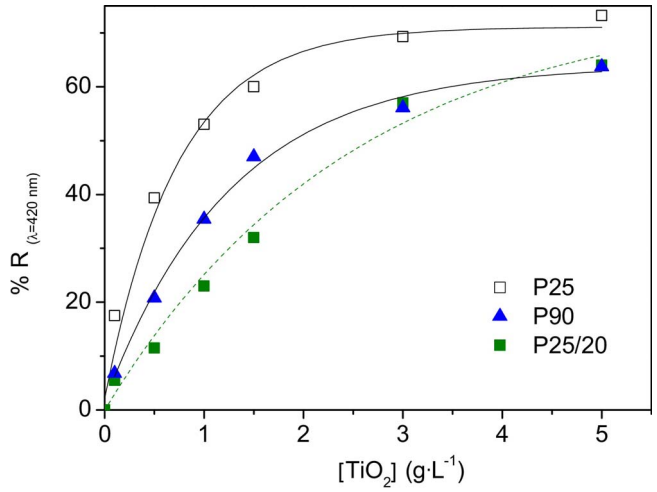

Fig. 5. Extinction of the light in function of the concentration of TiO_2 catalysts in aqueous suspension.

previously [26]. It can be seen that the lower the hydrodynamic particle size, the lower the radiation available at the center of the reactor because of higher scattering, absorption and albedo coefficients. That's why using concentrations close to 0.25 g L^{-1} is enough for P25 and P90 to achieve the maximum photodegradation rates whereas catalyst concentrations around 0.5–0.7 g L^{-1} are necessary when P25/20 is employed.

Finally, photocatalytic efficiency (Φ) has been evaluated for each optimal catalyst concentration and compared in function of hydrodynamic particle size for the same catalyst loading (see Table 1). Determinations were made following the model and procedure developed by Ballari et al. [28], who define photon efficiency in a photocatalytic system as the ratio between molar volumetric reaction rate (r) and the volumetric rate of photons absorption (VRPA), that is called photocatalytic efficiency (Φ) in the case of polychromatic radiation. In the case of same catalyst loading, although P90 has presented the maximum VRPA, higher recombination rates or other extinction reactions of photo-generated charges should be happening because of photocatalytic efficiency (Φ) was not corresponded, resulting P25 the most efficient photocatalyst. In contrast, P25/20 TiO_2 has given place to the lowest photo-efficiency. This behavior could be well explained by degree of aggregation of P25/20 TiO_2, characterized by hydrodynamic particle size distribution shifted to higher values in comparison with P25 (both catalysts have exactly presented same S_{BET} values). As discussed above, the lower hydrodynamic particle sizes of P25 catalysts should allow a better exposition to light radiation of titania particles surface in water suspension, while at the same catalyst loading, the access of the pollutant reactants to the internal particles of P25/20 TiO_2 becomes to be limited.

Photodegradation reactions and photocatalytic efficiencies performed at optimal catalyst loading, for comparative purpose, are also showed in Table 1, offered similar and optimal photocatalytic efficiency for these three titanium dioxides. Whereas P90 required a slightly higher loading than P25, more than double P25/20 loading was needed to lead similar photocatalytic efficiencies than optimal P25 catalyst loading. These results might be able to be applied to other catalysts, and could be expected, as pointed out in the literature, [23,35,37] that highly aggregated catalytic systems, with bigger hydrodynamic particle sizes, require higher catalyst loadings to achieve equivalent photocatalytic efficiency than less aggregated ones.

Table 2
Effect of sonication pre-treatment on titania exposed surface area.

Catalyst	Exposed surface area Without sonication pre-treatment ($m^2\ g^{-1}$)	Exposed surface area After sonication pre-treatment ($m^2\ g^{-1}$)
P25	0.61	3.78
P90	0.65	1.79
P25/20	0.08	2.34

3.3. Sonication pre-treatment on phenol photodegradation: Effect of TiO_2 hydrodynamic particle size

To go deeply in titania aggregation and disaggregation effects in aqueous suspensions along phenol photodegradation, initial phenol suspensions with their corresponding TiO_2 loadings were subjected to a sonication pre-treatment in dark conditions during 60 min.

An analysis of normalized kinetic parameters has been carried out to try to quantify in what way sonication pre-treatment is affected the photocatalytic process. In Table 2 are showed the effect of sonication pre-treatment on titania exposed surface area in reaction media, whereas in Fig. 6 are compared the normalized activities during phenol photo-oxidation for catalyst loadings of 250 mg L^{-1}; that correspond to calculated ratios of two kinetic parameters: phenol pseudo first-order constant and TOC initial photo-oxidation rate, where maximum kinetic parameters have always been assigned to TiO_2 P25.

After sonication pretreatment, at the same time that very higher exposed surface areas were found, not important changes in normalized kinetic parameters can be seen, except in the case of P25/20 catalyst. From Table 2 seems as though some aggregation and disaggregation phenomena could be occurring in the aqueous media during sonication pre-treatment, leading to a better exposition of the surface of aqueous suspended particles at irradiation light.

Hydrodynamic particle size distributions of sonicated TiO_2 photocatalysts in aqueous suspensions are showed in Fig. 7. Whereas TiO_2 catalysts with original mono-modal particle sizes (P25 and P90) have led to a bimodal distributions after sonication pre-treatment shifting to lower sizes at the same time that are kept their original ones, P25/20 has clearly presented an important disaggregation ($\approx$0.2 μm), besides their original bimodal distribution constituted by more aggregated particles $\approx$40 μm, and other minor corresponding to original P25 particle size (3–4 μm).

Probably, this disaggregation effect found in TiO_2 P25/20 particles after sonication pre-treatment, since the beginning of photocatalytic process, has been able to led to optimal photocatalyst conditions. Higher number of lower particles could provoke a global higher exposed surface in reaction media, where all of them can be perfectly illuminated and so, improving phenol photo-oxidation. Therefore, the

Table 1
Photon absorption rates (VRPA), initial phenol photodegradation rates and photocatalytic efficiency (Φ) in function of catalyst loading.

Catalyst	Catalyst loading (mg L^{-1})	VRPA (Einstein $L^{-1}\ min^{-1}$)	$(-r_{0,phenol})$ (mmol $L^{-1}\ min^{-1}$)	r^2	$\Phi = (-r_{0,phenol})$/VRPA (mmol $Einstein^{-1}$)
P25	250	2.27×10^{-4}	2.70×10^{-3}	0.970	11.89
P90	250	2.45×10^{-4}	2.82×10^{-3}	0.987	11.51
P25/20	250	2.07×10^{-4}	1.94×10^{-3}	0.994	9.37
P25	200	2.23×10^{-4}	2.73×10^{-3}	0.997	12.22
P90	250	2.45×10^{-4}	2.82×10^{-3}	0.987	11.51
P25/20	500	2.40×10^{-4}	3.09×10^{-3}	0.979	12.88

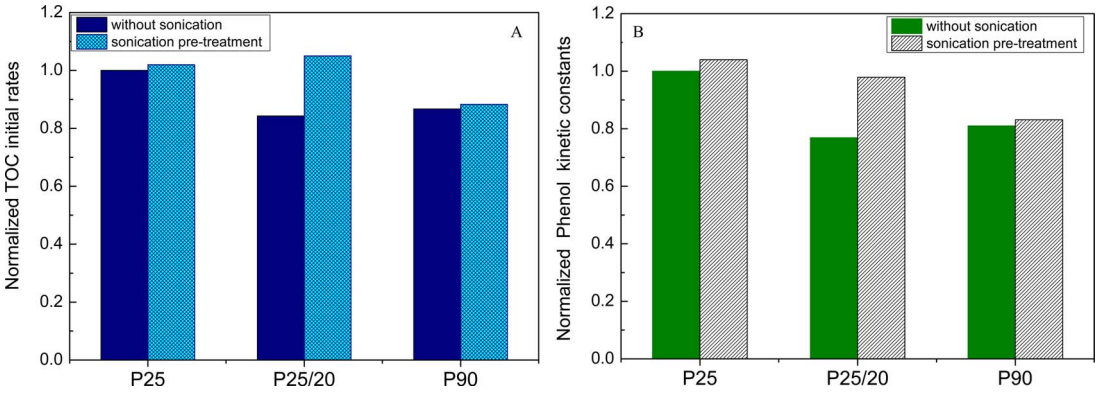

Fig. 6. Effect of sonication pre-treatment on normalized kinetic parameters: (A) $(-r_{0,TOC})/(-r_{0,TOC})_{Max}$ (B) $(k_{Phenol})/(k_{Phenol})_{Max}$.

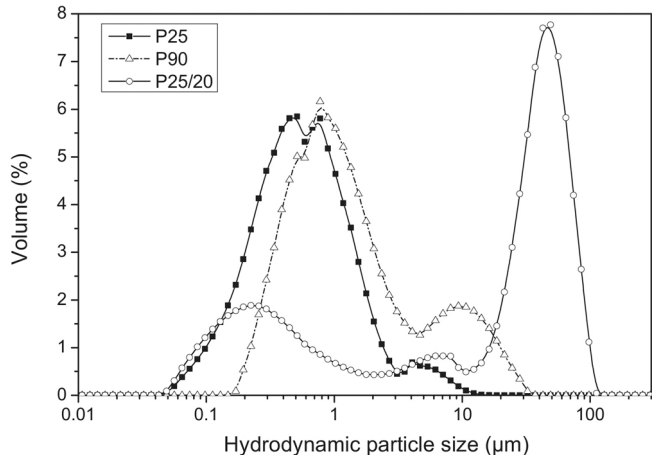

Fig. 7. Hydrodynamic particle size distributions of sonicated TiO_2 photocatalysts in aqueous suspensions.

presence of an important contribution of these lowest particles sizes (≈0.2 μm) found in sonicated P25/20 catalyst could well be responsible of significant improvements found in phenol photodegradation along irradiation time; as it can be seen in Fig. 8, where the effect of sonication pre-treatment on phenol concentration evolution is analyzed for catalyst loadings of 250 mg L^{-1}. In spite of the fact that P90 and P25 catalysts have not presented almost differences in the normalized kinetic parameters (see Fig. 6), noteworthy differences in the case of P25/20 TiO_2 as $(-r_{0,TOC})/(-r_{0,TOC})_{Max}$ as $(k_{Phenol})/(k_{Phenol})_{Max}$ are observed to compare original process with that from sonication pre-treatment. Where the presence of important disaggregation phenomena, found in P25/20 with very low hydrodynamic particle sizes, have led to reach the same phenol reduction that TiO_2 P25 at 300 min of irradiation time (see Fig. 8). This effect could be well explained by the presence of very low particle sizes in sonicated P25/20 catalyst which have considerably increased the value of total exposed surface area in aqueous media (see Table 2) leading to important improvements in phenol photodegradation. This phenomenon can only be related to hydrodynamic particle size distributions in aqueous suspensions, since P25 and P25/20 present the same structural, morphological, textural, chemical surface and electronic properties but with singular differences in aggregation and hydrodynamic particle size in aqueous media.

So, it can be said this disaggregation effect, found after sonication pre-treatment in P25/20 is playing an important role on their final photocatalytic efficiency.

Taking into account that a pollutant such as phenol, where photooxidation efficiency is regularly mediated by an indirect photo-mechanism via HO• radical, it seems important to reach a certain knowledge about hydroxyl radical production through both studied conditions: without and after sonication pre-treatment. In this context, aggregation effects of TiO_2 particles could be decisive along generation of free hydroxyl radicals in aqueous suspensions [38]. Thus, in Fig. 9 is given evolution of HO• for catalyst loadings of 250 mg L^{-1}, from the measured fluorescence emission area of 2-hydroxy terephthalic acid, along the irradiation time for all these studied TiO_2 in both conditions: without and with sonication pre-treatment. In general all of these TiO_2 catalysts have always presented two clear trends in HO• area evolution: first, a linear tendency directly proportional at shorter irradiation times (until 30 min), and after that, increases in irradiation times led to slightly increases in hydroxyl radicals areas.

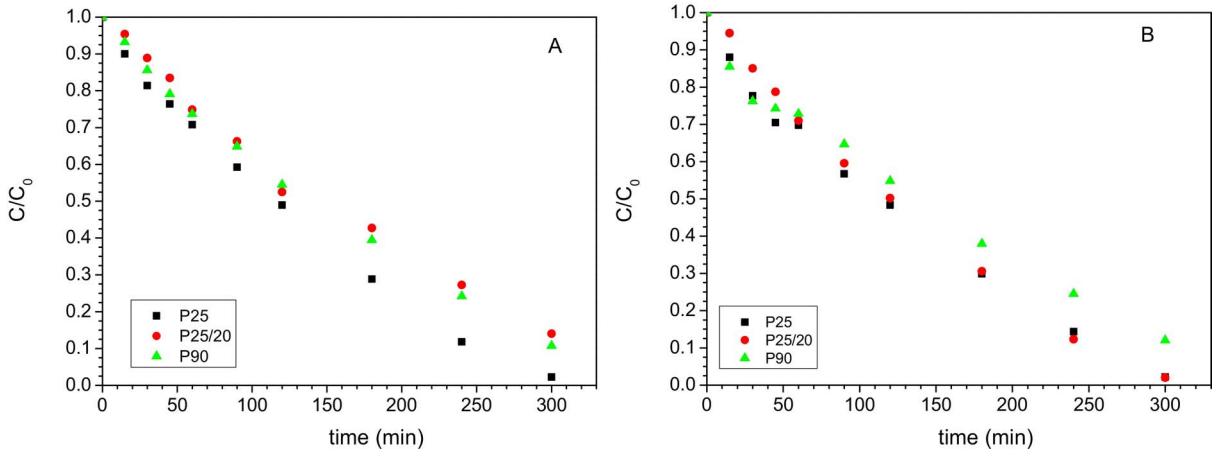

Fig. 8. Evolution of relative phenol concentrations without (A) and after sonication pre-treatment (B).

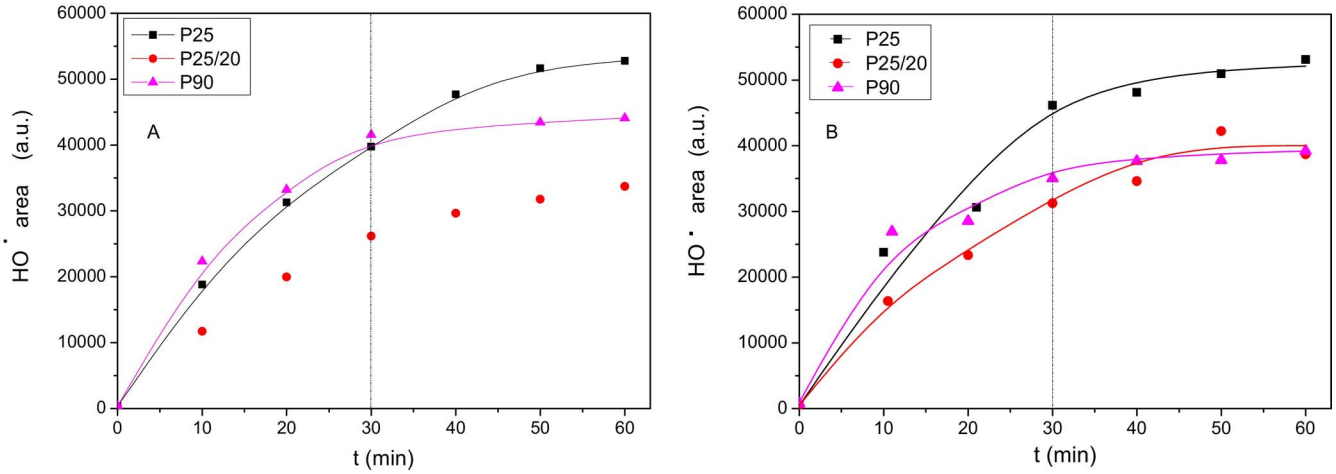

Fig. 9. Evolution of HO• radical generation without (A) and after sonication pre-treatment (B).

In the case of P90, in general after sonication a lower area of the fluorescence spectra has been observed. Although as it can be expected, slightly higher areas were noted until 10 min of irradiation time from that, smaller values were always observed. These singular results, maybe could be related to higher recombination rates or even other extinction reactions of photo-generated charges that could begin to be more important after sonication pre-treatment giving place to the lower detected hydroxyl radical generation, since although P90 catalysts presented the maximum VPRA (see Table 2), its photocatalytic efficiency (Φ) was not corresponded.

It can be emphasized that a higher hydroxyl radical production generated with P25/20 catalysts agrees with the important improvement of phenol removal found after sonication pre-treatment (see Fig. 9). In this line, whereas small differences in HO• production were found along irradiation time with P25 and P90, respectively, higher areas of fluorescence spectra of 2-hydroxyterephthalic acid after sonication pre-treatment were always observed in P25/20, as it can be seen in Supporting information Fig. 4.

4. Conclusions

The specific small differences of these Evonik TiO_2 catalysts made possible the analysis of their final photocatalytic efficiency, with a pollutant such as phenol, where photo-oxidation efficiency is regularly mediated by an indirect photo-mechanism via HO• radical.

Phenol photocatalytic efficiency attends P25 > P90 > P25/20 order, highlighting that radiation–photocatalyst interactions are essential but not enough to guarantee an improved photodegradation rate. Therefore, even though a complex correlation between the most relevant catalytic properties and reaction parameters usually governs heterogeneous photocatalytic processes, it can be emphasized that increases in these nanostructured TiO_2 hydrodynamic particle sizes are detrimental to phenol photocatalytic-efficiency.

Reflectance measurements in the range of visible wavelength close to TiO_2 absorption edge could be comparable to extinction coefficient in the UV-A range and may well be suitable to optimize catalyst loadings.

Lastly, the higher values of HO• area found in sonicated P25/20 catalyst could corroborate its better performance in phenol photodegradation, as a consequence of lowest hydrodynamic particle sizes ($\approx$0.2 μm) in the reaction media which take advantage of light as a result of a significant increase in exposed surface area.

Acknowledgments

This work has been supported by the Spanish Plan Nacional de I+D+i through the projects CTM2015-64895-R and CTM2016-76454-R. Jaime Carbajo thanks to the Spanish Ministerio de Economía y Competitividad (MINECO) for his FPI grant. Alvaro Tolosana-Moranchel thanks to Ministerio de Educación, Cultura y Deporte for his FPU grant (FPU14/01605). The authors are also grateful Evonik company for TiO_2 samples.

Appendix A. Supplementary data

Supplementary data associated with this article can be found, in the online version, at http://dx.doi.org/10.1016/j.apcatb.2017.08.032.

References

[1] V. Augugliaro, M. Litter, L. Palmisano, J. Soria, J. Photochem. Photobiol., C: Photochem. Rev. 7 (2006) 127.
[2] C. Adán, J. Carbajo, A. Bahamonde, I. Oller, S. Malato, A. Martínez-Arias, Appl. Catal., B: Environ. 108–109 (2011) 168.
[3] S. Malato, P. Fernandez-Ibáñez, M.I. Maldonado, J. Blanco, W. Gernjak, Catal. Today 147 (1) (2009) 147.
[4] R. Roy, S. Berger, P. Schmuki, Ang. Chem. Int. Ed. 50 (2011) 2904.
[5] J.M. Herrmann, Appl. Catal., B: Environ. 99 (2010) 461.
[6] J. Ryu, W. Choi, Environ. Sci. Technol. 42 (2008) 294.
[7] J. Ungelenk, C. Feldmann, Appl. Catal., B: Environ. 127 (2012) 11.
[8] A. Mills, J. Wang, D.F. Ollis, J. Catal. 243 (2006) 1.
[9] S.H. Lin, C.H. Chiou, C.K. Chang, R.S. Juang, J. Environ. Manage. 92 (2011) 3098.
[10] O.O. Prieto-Mahaney, N. Murakami, R. Abe, B. Ohtani, Chem. Lett. 38 (2009) 238.
[11] R. Enríquez, A.G. Agrios, P. Pichat, Catal. Today 120 (2007) 196.
[12] J. Sun, L.-H. Guo, H. Zhang, L. Zhao, Environ. Sci. Technol. 48 (2014) 11962.
[13] Y.X. Liu, G.X. Chen, A.A. Keller, C.M. Su, Environ. Sci.: Processes Impacts 15 (2013) 169.
[14] I. Chowdhury, D.M. Cwiertny, S.L. Walker, Environ. Sci. Technol. 46 (2012) 6968.
[15] L. Chowdhury, S.L. Walker, S.E. Mylon, Environ. Sci.: Process Impacts 15 (2013) 275.
[16] K.M. Reddy, S.V. Manorama, A.R. Reddy, Mater. Chem. Phys. 78 (2003) 239.
[17] A.E. Cassano, O.M. Alfano, Catal. Today 58 (2000) 167.
[18] B. Ohtani, O.O. Prieto-Mahaney, D. Li, R. Abe, J. Photochem. Photobiol., A: Chem. 216 (2010) 179.
[19] R. Jenkins, R.L. Zinder, Introduction to X-Ray powder Diffractometry, John Wiley & Sons Inc., New York, NY, 1996.
[20] S. Brunauer, P.H. Emmet, E. Teller, J. Am. Chem. Soc. 60 (1938) 309.
[21] O.M. Alfano, D. Bahnemann, A.E. Cassano, R. Dillert, R. Goslich, Catal. Today 58 (2000) 199.
[22] M.L. Satuf, L.J. Brandi, A.E. Cassano, O.M. Alfano, Ind. Eng. Chem. Res. 44 (2005) 6643.
[23] G. Plantard, T. Janin, V. Goetz, S. Brosillon, Appl. Catal., B: Environ. 115–116 (2012) 38.
[24] P. García-Muñoz, J. Carbajo, M. Faraldos, A. Bahamonde, J. Photochem. Photobiol., A: Chem. 8 (2014) 287.
[25] H.J. Kuhn, S.E. Braslavsky, R. Schmidt, Pure Appl. Chem. 76 (2004) 2105.
[26] A. Tolosana-Moranchel, J.A. Casas, J. Carbajo, M. Faraldos, A. Bahamonde, Appl. Catal., B: Environ. 164 (2017) 200.
[27] J. Marugan, R. Van Grieken, A.E. Cassano, O.M. Alfano, Catal. Today 129 (2007) 143.
[28] M.M. Ballari, O.M. Alfano, A.E. Cassano, Ind. Eng. Chem. Res. 48 (2009) 1847.
[29] M. Saran, K.H. Summer, Assaying for hydroxyl radicals: hydroxylated terephthalate

is a superior fluorescence marker than hydroxylated benzoate, Free Radical Res. 31 (5) (1999) 429–436.
[30] C. Adan, A. Martinez-Arias, M. Fernandez-Garcia, A. Bahamonde, Appl. Catal., B: Environ. 76 (2007) 395.
[31] A.J. Maira, K.L. Yeung, C.Y. Lee, P.L. Yue, C.K. Chan, J. Catal. 192 (2000) 185.
[32] P. Fernández-Ibáñez, S. Malato, F.J. de las Nieves, Catal. Today 54 (1999) 195.
[33] J. Carbajo, Thesis Dissertation: Application of Solar Assisted Photodegradation of Organic Pollutants in Aqueous Phase with Nanostructured Titania Catalysts, Universidad Autonoma de Madrid, Spain, 2013.
[34] S. Malato, J. Blanco, C. Richter, D. Curco, J. Jiménez, Water Sci. Technol. 35 (1997) 157.
[35] D. Vione, C. Minero, V. Maurino, M.E. Carlotti, T. Picatonotto, E. Pelizzeti, Appl. Catal., B: Environ. 58 (2005) 79.
[36] A. Tolosana-Moranchel, J.A. Casas, J. Carbajo, M. Faraldos, A. Bahamonde, Appl. Catal., B: Environ. 200 (2017) 7821.
[37] P. Saravanan, K. Pakshirajan, P. Saha, J. Hydro-environ. Res. 3 (2009) 45.
[38] D. Jassby, J.F. Budarz, M. Wiesner, Impact of aggregate size and structure on the photocatalytic properties of TiO_2 and ZnO nanoparticles, Environ. Sci. Technol. 46 (2012) 6491–6934.